03,16

Optical properties of phase-change materials of the GST system of the compositions $Ge_{14}Sb_{29}Te_{57}$ and $Ge_{15}Sb_{15}Te_7$ in the terahertz IR range

© V.A. Ryzhov[1], L.P. Kazakova[1,2], S.N. Garibova[3]

[1] Ioffe Institute,
St. Petersburg, Russia
[2] Kirov State Forest Technical University,
St. Petersburg, Russia
[3] Institute of Physics, National Academy of Sciences of Azerbaijan,
Baku, Azerbaijan

E-mail: v.ryzhov@mail.ioffe.ru

Received December 12, 2025
Revised December 24, 2025
Accepted December 24, 2025

Infrared absorption spectra of chalcogenide alloys of the GST system with the compositions $Ge_{20}Sb_{20.5}Te_{51}$, $Ge_{15}Sb_{15}Te_{70}$ and $Ge_{14}Sb_{29}Te_{57}$ in the amorphous and crystalline state were measured and analyzed in the range of $20-250\,cm^{-1}$ (0.6−12 THz) at room temperature. Absorption at these frequencies is due to the manifestation of correlated torsional vibrations of structural units of the amorphous alloy and phonon modes of the crystal. The performed assignment of absorption bands and the revealed differences in the IR spectra make it possible to more confidently represent the possible molecular mechanism of reversible amorphous-crystalline transformations in the studied phase-changing materials.

Keywords: chalcogenide alloys of the GST, GST-124 system, low-frequency IR spectra, phonons and Bose-peak, orientational phase transition.

DOI: 10.61011/PSS.2026.01.63236.344-25

1. Introduction

Chalcogenide ternary alloys Ge-Sb-Te have attracted much attention due to their ability to reversibly switch between the amorphous and crystalline phases [1–3]. The large contrast of physical properties (optical reflectivity, electrical conductivity, etc.) between these two phases makes it easy to read the nature of the phase, which was caused by various methods: thermal heating, electric current pulses, or optical pulses. Moreover, this switching process can be very fast (in the range of tens of ns), which opens up opportunities for the widespread use of triple GST alloys as active elements of non-volatile memory and allows them to be used to create rewritable CDs, DVDs, and discs Blu-ray [4].

The stable structure of GST is trigonal, but upon crystallization from the amorphous phase, GST crystallizes into a metastable cubic phase. Crystallization from the amorphous phase remains a time-limiting process in phase transition memory, and a detailed understanding and modeling of crystallization kinetics is crucial. Therefore, data on the structural properties of the GST system and the mechanism of the phase transition itself continue to accumulate and are actively discussed [5–9].

Thus, the extended X-ray absorption spectroscopy (EXAFS) method has shown that the local structure of the GST (distorted face-centered cubic lattice) does change during amorphization. The average Ge atom coordination value decreases from 6-fold in the crystal to 4-fold in the amorphous GST. Hence, it is concluded that the structural transition to GST is associated with the local environment of the Ge atom, which switches from an octahedral environment in the crystalline state with 6 nearest neighbors and binding angles of the order 90° to a tetrahedral environment with 4 nearest neighbors and binding angles of the order 109° [5]. This picture contradicts the interpretation of other EXAFS data [6], from which it follows that during the phase transition, the Ge atom remains in octahedral symmetry. At the same time, molecular dynamics modeling in amorphous GST shows [8,9] that the Ge atom indeed has a 4-fold coordination, but only a third of the Ge atoms are in a tetrahedral environment, whereas most Ge atoms and all Te and Sb atoms have a defective octahedral environment. And in the Raman spectrum, the tetrahedral structure should appear at frequencies above $190\,cm^{-1}$, whereas the main peaks at ~ 120 and $\sim 140\,cm^{-1}$ should be attributed to the manifestation of atomic vibrations in defective octahedra [10]. This means that, apart from calculations, experimental evidence for the identification of tetrahedral Ge in amorphous GST has not yet been presented.

The dramatic differences in physical properties between the amorphous and crystalline GST systems are explained not only by a change in the geometry (coordination) of the environment, but also by a change in the nature of the covalent chemical bond in the amorphous and resonant in the crystalline phase [11]. The role of high

defect concentration is also considered [12] and Peierls are distortions in the octahedral medium of Ge atoms[13].

Compared to the modern methods of studying the local atomic structure and interactions in GST presented above, infrared (IR) spectroscopy is used less frequently. Only two papers have been published [14,15] with IR absorption spectra of GST system materials at the same frequencies as in the Raman spectra, which are mainly used to draw conclusions about the molecular mechanism of the phase transition in this system [16]. The use of IR spectroscopy, which has extensive experience in interpreting the vibrational spectra of crystalline and amorphous substances, seems completely natural both for determining the structure of the short-range order and for studying the dynamics of individual structural units and their interrelationships [17], especially in the terahertz range, where multiphonon absorption in short-range groups is manifested, as well as lattice absorption in a crystal and absorption induced by disorder in an amorphous medium [18].

The aim of this study was to obtain IR transmission spectra in the region of $20-250\,\mathrm{cm}^{-1}$ ($0.6-7\,\mathrm{THz}$) alloys of the GST system containing 20, 15 and 14 at.% germanium, 20.5, 15 and 29 at.% antimony, 51, 70 and 57 at.% tellurium ($Ge_{20}Sb_{20.5}Te_{51}$, $Ge_{15}Sb_{15}Te_{70}$ and $Ge_{14}Sb_{29}Te_{57}$, respectively) in an amorphous and crystalline state. The obtained spectra were analyzed based on calculations and published data. The results were interpreted in terms of lattice vibrations (phonons) in the crystalline and torsion-vibrational dynamics in the amorphous state of the alloy. The assignment of absorption bands makes it possible to more confidently imagine the possible molecular mechanism of reversible amorphous-crystalline transformations in the studied materials.

2. Samples and experimental procedure

The samples of $Ge_{15}Sb_{15}Te_{70}$ and $Ge_{14}Sb_{29}Te_{57}$ were prepared by melt quenching in vacuumed sealed quartz ampoules (residual pressure $\sim 10^{-3}\,\mathrm{Pa}$). Synthesis took place at a temperature of 950 °C for 6 h at a heating rate of 3–4°C/min. In the synthesis process, the melt was repeatedly mixed to homogenize it. The peculiarity of the synthesis of $Ge_{14}Sb_{29}Te_{57}$ was that it was carried out in vacuumed sealed quartz ampoules with an elongated conical end [19]. This made it possible to estimate the glass-forming ability of the melt by the size of the cone cross-section diameter. $Ge_{14}Sb_{29}Te_{57}$ melt was also cooled in the quenching mode. X-ray phase analysis showed that the main phase is diffractometrically close to $Ge_{0.95}Sb_{2.01}Te_4$ with hexagonal cell parameters $a = 4.23\,\text{Å}$ and $c = 41.1\,\text{Å}$. An admixture of eutectic (Sb, Te) can be present in a hardened sample.

Figure 1 shows X-ray images of alloys of $Ge_{14}Sb_{29}Te_{57}$ and $Ge_{15}Sb_{15}Te_{70}$ which were rapidly cooled and thermally annealed at 200 °C, as well as angular distributions of the intensity of X-ray diffraction of $Ge_{20}Sb_{20.5}Te_{51}$ at room temperature.

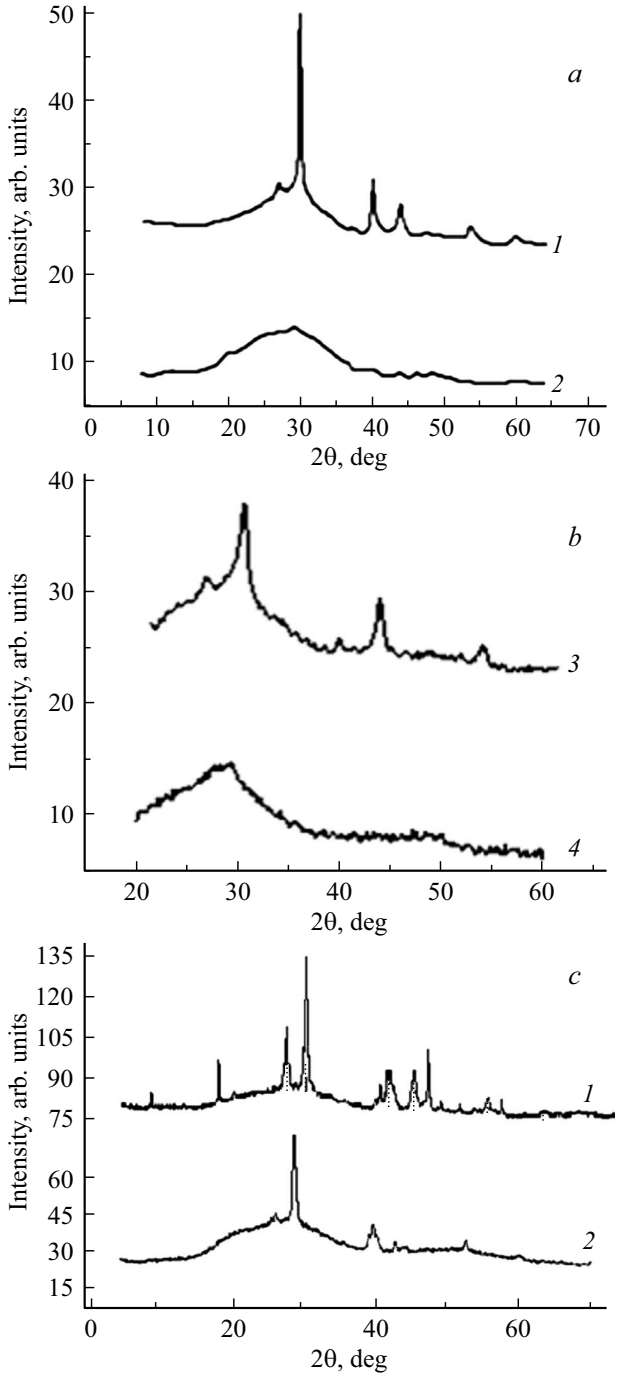

Figure 1. *a* and *b* — X-ray spectra of alloys of $Ge_{14}Sb_{29}Te_{57}$ (curves *1, 2*) and $Ge_{15}Sb_{15}Te_{70}$ (*3, 4*). X-ray scanning of alloys hardened in liquid nitrogen (*2, 4*). X-ray scanning of thermally annealed alloys at 200 °C (*1, 3*). *c* — angular intensity distributions of X-ray diffraction of $Ge_{20}Sb_{20.5}Te_{51}$: at room temperature (curve *1* — volume sample before heat treatment, *2* — after heat treatment).

The X-ray image of the rapidly hardened samples shows the amorphous nature of the alloy, since there are no

noticeable peaks on it, whereas the X-ray image of the samples after annealing shows their polycrystalline nature.

The chalcogenide semiconductor $Ge_{20}Sb_{20.5}Te_{51}$ was obtained by fusing high purity elementary substances in quartz ampoules vacuumed to 10^{-4} mm Hg. The synthesis was carried out at a temperature of 900 °C for 10 h, with an exposure for at least 5 h in a rotating thermostat, followed by cooling in the off thermostat mode. Volumetric samples with a thickness of 1.5 mm were used as measurement samples. Figure 1, *c* shows X-ray images of $Ge_{20}Sb_{20.5}Te_{51}$ at room temperature and after heat treatment. The presence of peaks at room temperature indicates the presence of a crystalline structure in the bulk image.

The alloys obtained in this way were ground to a powder form for analysis. IR transmission spectra in the region of 150–250 cm^{-1} were recorded using a Hitachi FIS-21 spectrometer. The spectra in the region of 20–150 cm^{-1} were recorded using a spectrometer developed at St. Petersburg State University and upgraded at Physical-Technical Institute with an OAP-7 receiver and a new filtration system. The resolution with a signal-to-noise ratio of the order of 100 was 1–2 cm^{-1}. The measurements were performed using the method of polyethylene tablets. Amorphous and polycrystalline samples were carefully ground to an average particle size of 10–15 μm in dry argon to eliminate surface oxidation. All spectra were taken at room temperature.

The Raman spectra were studied on a three-dimensional confocal Raman microscope Nanofinder 30 (Tokyo Instr.), the excitation wavelength was 532 nm. The cross-sectional radius of the laser beam incident on the film was $\sim 4\,\mu$m. The radiation receiver was a cooled CCD camera (−70 °C) operating in photon counting mode, the exposure time was 10–40 s with a laser radiation power of 9 mW, spectral resolution error was 0.5 cm^{-1}.

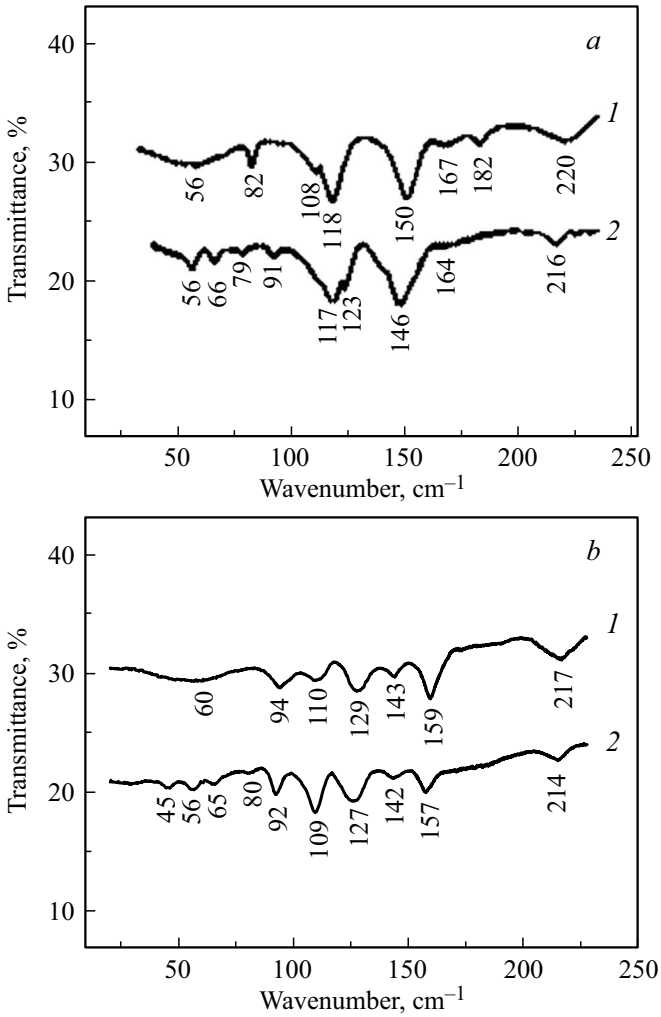

Figure 2. IR transmission spectra of GST system alloys: *a* — spectra of alloy $Ge_{14}Sb_{29}Te_{57}$; *b* — spectra of alloy $Ge_{15}Sb_{15}Te_{70}$. Curves *1* — in the amorphous, *2* — in the crystalline state.

3. Results and their discussion

Figure 2 shows the low-frequency IR transmission spectra of polycrystalline and amorphous GST materials $Ge_{15}Sb_{15}Te_{70}$ and $Ge_{14}Sb_{29}Te_{57}$ in the range 20–250 cm^{-1}.

Figure 3 shows the low-frequency IR transmission spectra of a partially crystalline GST material $Ge_{29}Sb_{20}Te_{51}$ in the range of 20–250 cm^{-1}.

It can be seen that the spectra of the presented alloys in the amorphous and crystalline states at frequencies above 100 cm^{-1} are almost identical. Their main difference is in the range of external vibrational modes: in amorphous samples, instead of bands of the crystal lattice, there is one abnormally wide absorption band.

The IR transmission spectra of GST alloys $Ge_{20}Sb_{20}Te_{51}$ in the wavelength range from 20 to 250 cm^{-1} represent a structureless plateau, against which it is possible to distinguish several peaks of overlapping absorption bands. The most intense of them in the spectra of crystalline samples occur at 51, 66, 79, 96, 117, 123 148, 164, 183, 215 cm^{-1} and at 45, 56, 66, 86, 92, 109, 127, 142, 152, 214 cm^{-1} in the spectra of partially crystalline („massive“) samples, respectively. The bands are slightly (by 2–3 cm^{-1}) shifted to high frequencies and redistributed in intensity in the „spectra of massive“ samples.

The assignment of bands in the presented spectra was carried out based on a calculation in which the GST alloy was considered as a spatially three-dimensional inorganic polymer having a composition in the form of two covalently constructed structural units of short-range regions: $GeTe_4$ tetrahedra and Sb_2Te_3 trigonal pyramids. The identity of the vibrational spectra of simple molecules and the spectra of solids containing the same or similar structural groups justifies this approach [20].

The pentatomic tetrahedral „molecule“ of $GeTe_4$, crystallizing in Td symmetry, has 15 active IR and Raman mobility modes, including 3 rotational and 3 translational modes. The active IR modes will be 2 acoustic symmetry modes A1u and Eu and 4 optical modes 2A1u and 2Eu. For the center of the Brillouin band, the complete representation

Normal oscillation frequencies of $GeTe_4$ and $SbTe_3$ in the phonon spectra of the GST alloy compositions $Ge_{15}Sb_{15}Te_{70}$, $Ge_{14}Sb_{29}Te_{57}$ and $Ge_{20}Sb_{20}Te_{51}$

Sample	Normal oscillation frequencies, cm^{-1}									
	$\nu_1(A_1)^*$		$\nu_2(E)$		$\nu_3(F_2)$		$\nu_4(F_2)$		$\nu_r(F_1)$	
	$GeTe_4$	$SbTe_3$	$GeTe_4$	$SbTe_3$	$GeTe_4$	$SbTe_3$	$GeTe_4$	$SbTe_3$	$GeTe_4$	$SbTe_3$
$GeTe_4$ [15]	125	–	87	–	209	–	78	–	60	–
$SbTe_3$ [16]	–	164	–	122	–	145		106	–	53
$Ge_{15}Sb_{15}Te_{70}$ [23]	117	148	96	123	216	148	79	96	66	56
$Ge_{14}Sb_{29}Te_{57}^{**}$	109	152	92	127	214	142	80	92	66	45
$Ge_{20}Sb_{20}Te_{51}$	110	165	92	117	225	149	81	92	65	51

Note. * ν_1 and ν_3 — valence modes of symmetric and antisymmetric oscillations, ν_2 and ν_4 — symmetric and antisymmetric deformation modes mods, ν_r and ν_t — external mods for free rotation and translation. ** Data of this study.

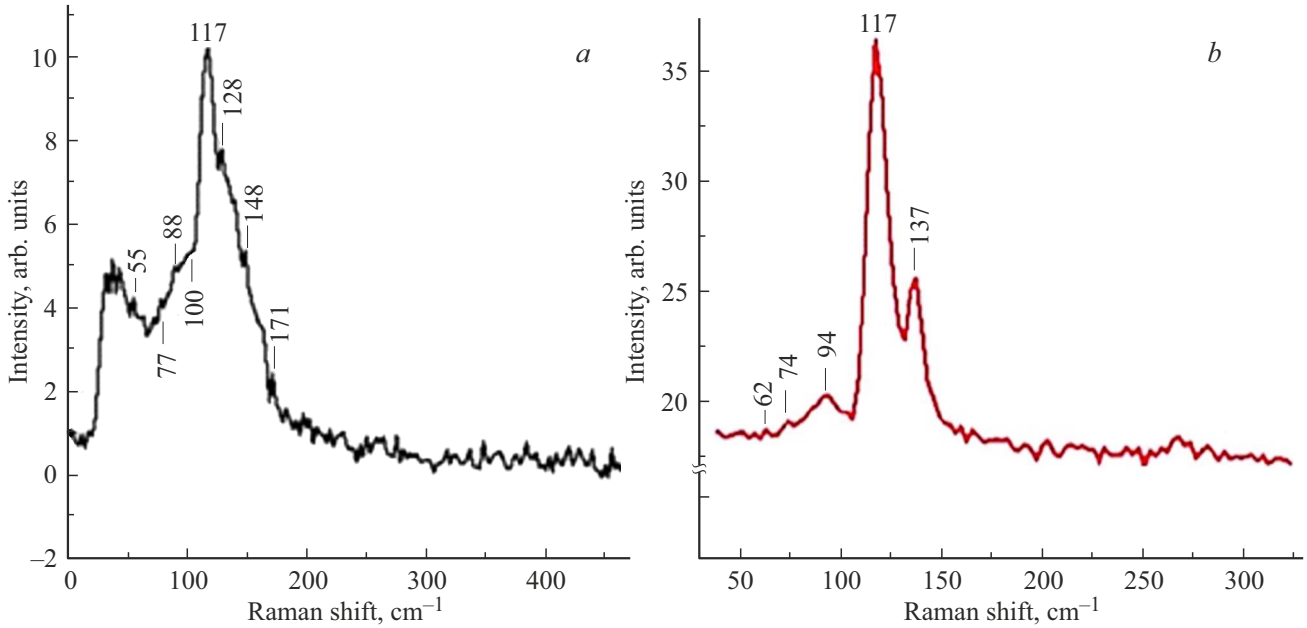

Figure 4. Raman spectra of the bulk sample $Ge_{20}Sb_{20}Te_{51}$: *a* — before heat treatment, *b* — after heat treatment.

is expressed as G = A1 + E + F1 + 3F2, where modes A1 and E correspond to intramolecular valence and deformation vibrational modes Au and Eu, and modes F1 and F2 — external, rotational (libration) mode F1(ν_r) and translational mode F2 (ν_t). The A1 + E + 2F2 modes, usually denoted as ν_1, ν_2, ν_3 and ν_4, respectively, are internal modes of $GeTe_4$ tetrahedra GST alloys. The modes predicted by group theory for tetrahedral symmetry and the calculated phonon frequencies at the point G(Td) are shown in the table; as can be seen from the table, they are consistent with the assignment of bands in the spectrum of GeI_4 [21,22], which is close in mass ratio to $GeTe_4$.

It is also seen that due to violations of the selection rules, other predicted fundamental modes appear in the IR spectra of GeX_4 molecules, in addition to the IR active modes ν_3 and ν_4, confirming that the crystallinity of the GST alloy is imperfect [2].

The tetraatomic molecule $SbTe_3$ crystallizes in a structure with C3v symmetry and has 12 phonon modes, including external R and T modes for the wave vector *K*. For $K = 0$, group-theoretic analysis provides the following complete representation: G(C3v) = 2A1g + 2A1u + 2Eg + 2Eu, including acoustic IR and Raman modes: G_a = A1u + Eu, G_R = 2A1g + 2Eg and G_{IR} = A1u + Eu, where A1u corresponds to pure rotation (ν_r), and Eu corresponds to pure translation (ν_t). The valence modes are designated as ν_1 and ν_3 for fully symmetric and antisymmetric oscillations, respectively. The deformation modes are designated as ν_2(A1) and ν_4(E). All these four oscillations are both IR and Raman active.

The modes predicted by the group theory for pyramidal symmetry and the phonon frequencies calculated on its basis at the point G(C3v) are given in the table. They are in good agreement with the position of the bands in the SbI_3 spectrum [24], which makes it possible to confidently attribute phonon frequencies for $SbTe_3$. The relation shown in the table is confirmed by comparing the ratio between the frequencies of the valence (ν_3/ν_1) and deformation (ν_4/ν_2)

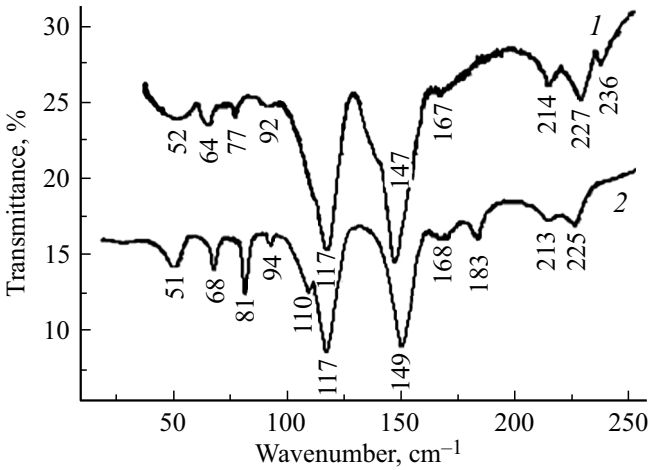

Figure 3. IR transmission spectra of an alloy of the GST system $Ge_{29}Sb_{20}Te_{51}$: curve *1* — in partially crystalline, *2* — in crystalline condition.

modes for SbI_3 with similar values obtained during the calculation. It can be seen that these frequency ratios are almost the same for SbI_3 and $SbTe_3$.

The assignment of IR bands in the spectra of crystalline compositions $Ge_{15}Sb_{15}Te_{70}$ and $Ge_{14}Sb_{29}Te_{57}$, shown in the table, is comparable to the frequency assignment known from the literature [25,26] in the Raman spectra of GST materials. Thus, the most intense bands in the Raman spectra at 117 and 157 cm^{-1} in cubic $Ge_{22}Sb_{22}Te_{56}$ (GST 225) were associated with valence modes of $GeTe_4$ tetrahedra and $SbTe_3$ pyramids, respectively. Figure 4 shows the Raman spectra of $Ge_{20}Sb_{20}Te_{51}$ before and after heat treatment at 400 °C.

The spectrum of the volumetric sample at room temperature consists of a wide band covering the frequency range 75−175 cm^{-1}, with weak maxima at 88, 148 and 171 cm^1. The maxima at 62, 74, and 94 cm^{-1} in the spectrum of the heat-treated sample are represented in the spectrum of the bulk sample by a wide band with a maximum at $\sim$ 50 cm^{-1}, while the maxima at 117 and 74−90 cm^{-1} are present in the spectrum of all samples.

The papers in Refs. [25,27–32] devoted to the study of the features of the Raman spectra of amorphous and crystalline samples of $Ge_{20}Sb_{20}Te_{51}$ attributed the peak 117 cm^{-1} to fluctuations of defective octahedral structural elements based on Ge. The band localized at a frequency of 150 cm^{-1} (in our studies at 147 cm^{-1}) is directly related to the structural element Sb_2Te_3 and is partially related to the pyramidal the structural element $SbTe_3$ [27]. In studies, the band with maxima 145−150 cm^{-1} was associated with fluctuations in the Sb−Te bond in the pyramidal structural element $SbTe_3$ [18] or in octahedrally coordinated atoms of Sb [31]. A wide band at 137 cm^{-1} was also observed in Ref. [33] and was associated with fluctuations in the homeopolar coupling of Te−Te. The authors of this work noted that this band is observed only in samples subjected to low-temperature annealing. The peak at 137 cm^{-1}, corresponding to the bond stretching modes Te−Te, did not appear in the Raman spectrum of bulk samples $Ge_{20}Sb_{20}Te_{51}$ [29], which was considered a sign of good crystallization.

The calculation performed in the study clarifies that the band with a maximum at 127 cm^{-1} (oscillation ν_1(A1) $GeTe_4$) also contributes to the mode ν_2(Eu) $SbTe_3$, whereas the frequency range of 85−115 cm^{-1} in the IR spectra is formed by at least two bands at $\sim$ 90 and 100 cm^{-1}, which, according to the calculation, were attributed to the deformation modes ν_2(E) and ν_4(F2) $GeTe_4$ and $SbTe_3$, respectively. The peak at $\sim$ 215 cm^{-1}, can probably be attributed to the mode ν_3(F2) — an asymmetric stretching oscillation of the $GeTe_4$ tetrahedron. A similar assignment of this peak in the Raman spectrum of crystalline GeTe (isostructured $Ge_{22}Sb_{22}Te_{56}$) was made in Ref. [34]. Bands with maxima at 92 and 142 cm^{-1}, which were assigned here to the modes ν_2(E) and ν_3(E) of $GeTe_4$ and $SbTe_3$ accordingly, in the IR spectrum of $Ge_{15}Sb_{15}Te_{70}$ — compounds with increased tellurium content — may also have a contribution of fragments consisting only of tellurium atoms [35].

The assignment of bands in the IR spectra of the studied polycrystalline alloys was used to assign bands in the spectra of the same alloys in an amorphous (glassy) state. Since the spectra of crystalline and amorphous alloys (as can be seen from Figure 2, *a*, curves *1* and *2*, and 2, *b*, curves *1* and *2*), do not differ much from each other, especially at $\nu > 100$ cm^{-1}, where intramolecular modes of structural units are manifested.

Since the crystalline phase is more ordered than the amorphous one, this fact shows the unusual similarity of the amorphous and short-range crystalline structures in the studied GST systems, and leads to the conclusion that there is a similar degree of topological disorder between these two states. That is, the local architecture of the tetrahedra and pyramids of the GST system remains unchanged during the phase transition.

At the same time, the analysis of Figures 2 and 3 shows that the phase transition leads to radical changes in the IR spectra of the studied GST at frequencies below 70 cm^{-1}, where fluctuations associated with the external degrees of freedom of the structural units of the crystal are manifested.

According to calculations, absorption peaks at 79, 66 and 56 cm^{-1} in the spectrum of crystalline $Ge_{15}Sb_{15}Te_{70}$ and at 80, 66 and 45 cm^{-1} in the spectrum of crystalline $Ge_{14}Sb_{29}Te_{57}$ — these are modes ν_t(F2), ν_t(F1) and ν_r(F1), due to the manifestation of torsional vibrations (librations) and translations of tetrahedra and pyramids.

In IR spectra of amorphous alloys $Ge_{15}Sb_{15}Te_{70}$, $Ge_{14}Sb_{29}Te_{57}$ and $Ge_{20}Sb_{20}Te_{51}$ in the same frequency range — only one abnormally wide band with a maximum at $\sim$ 60 cm^{-1}, which can be confidently It is attributed to the Bose peak in the low-frequency IR [36] and Raman spectra [14,15,37] of amorphous solids.

The origin of the Bose peak in the IR and Raman spectra of amorphous solids is associated with a violation of the

selection rules and an increase in the density of vibrational states during amorphization [36]. With the loss of long-range order, the system of coupled harmonic oscillators (phonons of the type ν_t(F2) and ν_r(F1)) becomes a system of misdirected anharmonic oscillators that retain only limited correlation, i. e., the average order, at scales of 10−30 Å [37]. The attribution of the Bose peak to the manifestation of this correlated torsional-vibrational motion (libration) of several molecular groups is discussed in Refs. [19,38].

Thus, while there is no data on the contrast of local structures between phases in the IR spectra of polycrystalline and amorphous GST materials in the range where *intramolecular* modes are manifested, the presence of a Bose peak at the frequencies of *intermolecular* modes directly indicates the existence of medium-order amorphous alloys, similar to the crystalline one, but without the orientational order.

The changes in the spectra revealed at terahertz frequencies suggest the following scenario of phase transition in GST alloys: inherent in „tetrahedral" and „pyramidal" structural units in these alloys, local distortions contribute to the formation of Ge−Ge and Ge−Sb bonds [39]. The correlated librations of these structures with a significant proportion of vacancies lead to the formation of an average (chain) order in the system. (This is evidenced by the presence of a Bose peak in the IR spectra). The transition of such a GST system to an ordered state does not require the breaking of chemical bonds and the restructuring of local structures; it is sufficient to reorient the existing blocks.

Such an order-disorder transition is, in fact, a relaxation transition according to the mechanism of fast Johari-Goldstein β-relaxation [40]. Such a transition is realized by overcoming minimal potential barriers and with minimal relaxation time.

4. Conclusion

The IR transmission spectra of polycrystalline and glassy materials of the GST system $Ge_{15}Sb_{15}Te_{70}$, $Ge_{14}Sb_{29}Te_{57}$ and $Ge_{20}Sb_{20}Te_{51}$ were measured in this study in the spectral range of 20−250 cm^{-1} at room temperature, and were also analyzed based on calculations and literature data.

The assignments made and the differences in the spectra of amorphous and crystalline samples revealed suggest the following probable molecular mechanism of reversible amorphous-crystalline transformations in GST alloys. According to most existing models, the presence of a Bose peak in the low-frequency IR and Raman spectra is a sign of the presence of a medium order in the structure of an amorphous body due to the correlated torsional-oscillatory motion (libration) of fragments of this structure. These fragments of the medium-order structure can play the role of crystallization centers at the nano-scale, and their libration can be considered as preceding the appearance of phonons in the crystal.

In accordance with this model, the crystallization of the amorphous phase is carried out by thermal reorientation of randomly oriented structural fragments, providing them with an energetically favorable position and long-range order of the system. In this case, GST crystallization does not affect the entire covalent network, but is more similar to the so-called β-relaxation, when only fragments of it relax. This process does not require large atomic displacements and occurs with a nanosecond relaxation time.

Conflict of interest

The authors declare that they have no conflict of interest.

References

[1] T. Ohta, S.R. Ovshinsky. In: Photo-induced Metastability in Amorphous Semiconductors / Ed. A.V. Kolobov. Berlin, Wiley-VCH (2003). Ch. 18.
[2] A.V. Kolobov, J. Tominaga. Chalcogenides: Metastability and Phase Change Phenomena. Berlin, Springer-Verlag (2012).
[3] F.C. Mocanu, K. Konstantinou, T.H. Lee, N. Bernstein, V.L. Deringer, G. Csányi, S.R. Elliott. J. Phys. Chem. B **122**, *38*, 8998 (2018).
[4] D. Lencer, M. Salinga, M. Wuttig. Adv. Mater. **23**, *18*, 2030 (2011).
[5] A.V. Kolobov, P. Fons, A.I. Frenkel, A.L. Ankudinov, J. Tominaga, T. Uruga. Nature Mater. **3**, *10*, 703 (2004).
[6] D.A. Baker, M.A. Paesler, G. Lucovsky, S.C. Agarwal, P.C. Taylor. Phys. Rev. Lett. **96**, *25*, 255501 (2006).
[7] S. Kohara, K. Kato, S. Kimura, H. Tanaka, T. Usuki, K. Suzuya, H. Tanaka, Y. Moritomo, T. Matsunaga, N. Yamada, Y. Tanaka, H. Suematsu, M. Takata. Appl. Phys. Lett. **89**, *20*, 201910 (2006).
[8] S. Caravati, M. Bernasconi, T.D. Kühne, M. Krack, M. Parrinello. Appl. Phys. Lett. **91**, *17*, 171906 (2007).
[9] J. Akola, R.O. Jones. Phys. Rev. B **76**, *23*, 235201 (2007).
[10] R. Mazzarello, S. Caravati, S. Angioletti-Uberti, M. Bernasconi, M. Parrinello. Phys. Rev. Lett. **104**, *8*, 085503 (2010).
[11] K. Shportko, S. Kremers, M. Woda, D. Lencer, J. Robertson, M. Wuttig. Nature Mater. **7**, *8*, 653 (2008).
[12] M. Wuttig, D. Lusebrink, D. Wamwangi, W. Welnic, M. Gilleben, R. Dronskowski. Nature Mater. **6**, *2*, 122 (2007).
[13] J.Y. Raty, V. Godlevsky, P. Ghosez, C. Bichara, J.P. Gaspard, J.R. Chelikowsky. Phys. Rev. Lett. **85**, *9*, 1950 (2000).
[14] K.V. Shportko, E.F. Venger. Nanoscale Res. Lett. **10**, *1*, 33 (2015).
[15] V. Bragaglia, K. Holldack, J.E. Boschker, F. Arciprete, E. Zallo, T. Flissikowski, R. Calarco. Sci. Rep. **6**, *1*, 28560 (2016).
[16] K.S. Andrikopoulos, S.N. Yannopoulos, G.A. Voyiatzis, A.V. Kolobov, M. Ribes, J.J. Tominaga. J. Phys.: Condens. Matter **18**, *3*, 965 (2006).
[17] K.D. Möller, W.G. Rothshild. Far Infrared Spectroscopy. Wiley-Interscience, N.Y. (1971).
[18] V.S. Libov, T.S. Perova. Nizkochastotnaya spektroskopiya mezhmolekulyarnyh vzaimodejstvij v kondensirovannyh sredah. Trudy GOI (in Russian) **81**, *215*, 3 (1992).
[19] V.B. Voloshinov, N. Gupta, L.A. Kulakova, V.S. Khorkin, B.T. Melekh, G.A. Knyazev. J. Opt. **18**, *2*, 025402 (2016).

[20] A. Feltz. Amorphe und glasartige anorganische Festkörper. De Gruyter, Berlin/Boston (1983).
[21] H. Stammreich, R. Forneris, Y. Tavares. J. Chem. Phys. **25**, *3*, 580 (1956).
[22] M.L. Delwaulle. Comptes Rendus Acad. Sci. **238**, *1*, 84 (1954).
[23] V.A. Ryzhov, B.T. Melekh. Semiconductord **52**, *2*, 209 (2018).
[24] W.Z. Kiefer. Z. Naturforsch. **25a**, 1101 (1970).
[25] P. Němec, V. Nazabal, A. Moreac, J. Gutwirth, L. Beneš, M. Frumar. Mater. Chem. Phys. **136**, *2–3*, 935 (2012).
[26] S. Kozyukhin, M. Veres, H.P. Nguyen, A. Ingram, V. Kudoyarova. Phys. Procedia **44**, 82 (2013).
[27] K. Shportko, L. Revutska, O. Paiuk, J. Baran, A. Stronski, A. Gubanova, E. Venger. Opt. Mater. **73**, 489 (2017).
[28] B. Liu, Z. Song, T. Zhang, S. Feng, B. Chen. Chinese Phys. **13**, *11*, 1947 (2004).
[29] E. Cho, S. Yoon, H.R. Yoon, W. Jo. J. Korean Phys. Soc. **48**, *6*, 1616 (2006).
[30] G.C. Sosso, S. Caravati, R. Mazzarello, M. Bernasconi. Phys. Rev. B **83**, *13*, 134201 (2011).
[31] S.A. Kozyukhin, V.H. Kudoyarova, H.P. Nguyen, A. Smirnov, V. Lebedev. Physica Status Solidi C **8**, *9*, 2688 (2011).
[32] G. Bulai, O. Pompilian, S. Gurlui, P. Nemec, V. Nazabal, N. Cimpoesu, B. Chazallon, C. Focsa. Nanomaterials (Basel) **9**, *5*, 676 (2019). doi: 10.3390/nano9050676.
[33] J. Tominaga, N. Atoda. Jpn. J. Appl. Phys. **38**, *3B*, L322 (1999).
[34] M. Upadhyay, S. Murugavel, M. Anbarasu, T.R. Ravindran. J. Appl. Phys. **110**, *8*, 083711 (2011).
[35] P. Grosse, W. Richter. In: Landolt-B ornstein: Numerical Data and Functional Relationships in Science and Technology, v. 17 / Ed. O. Madelung. Springer, Berlin (1983).
[36] M. Naftaly, E.R. Miles. J. Non-Cryst. Solids **351**, *40–42*, 3341 (2005).
[37] G.P. Johari. J. Non-Cryst. Solids **307–310**, 114 (2002).
[38] J. Baran, N.A. Davydova, A.J. Pietraszko. Mol. Struct. **744–747**, 301 (2005).
[39] A.V. Kolobov, M. Krbal, P. Fons, J. Tominaga, T. Uruga. Nature Chem. **3**, *4*, 311 (2011).
[40] G.P. Johari. J. Non-Cryst. Solids **307–310**, 317 (2002).

Translated by A.Akhtyamov